CHARACTERISATION OF URANIUM-¾ % TITANIUM
ALLOYS EXTRUDED FROM THE GAMMA PHASE

FINAL REPORT

by

R.I. Saunderson and G.B. Brook

R812/4/June 1981

Contract Number DAJA 37-79-C-0100 R&D 2622

S. T. h

R&D 2622-MS

SECURITY CLASSIFICATION OF THIS PAGE (When Data Entered)

REPORT DOCUMENTATION PAGE	READ INSTRUCTIONS BEFORE COMPLETING FORM

1. REPORT NUMBER	2. GOVT ACCESSION NO. AD-A103 651	3. RECIPIENT'S CATALOG NUMBER

4. TITLE (and Subtitle) Characterisation of Uranium-¾% Titanium Alloys Extruded from the Gamma Phase.	5. TYPE OF REPORT & PERIOD COVERED Final Technical Report
	6. PERFORMING ORG. REPORT NUMBER

7. AUTHOR(s) R. I. Saunderson and G. B. Brook	8. CONTRACT OR GRANT NUMBER(s) DAJA37-79-C-0100

9. PERFORMING ORGANIZATION NAME AND ADDRESS Fulmer Research Institute Limited Stoke Poges Slough, UK	10. PROGRAM ELEMENT, PROJECT, TASK AREA & WORK UNIT NUMBERS IT161102BH57H04

11. CONTROLLING OFFICE NAME AND ADDRESS USARDSG-UK Box 65 FPO NY 09510	12. REPORT DATE June 1981
	13. NUMBER OF PAGES 42

14. MONITORING AGENCY NAME & ADDRESS(If different from Controlling Office)	15. SECURITY CLASS. (of this report) Unclassified
	15a. DECLASSIFICATION/DOWNGRADING SCHEDULE

16. DISTRIBUTION STATEMENT (of this Report)

Approved for Public Release - Distribution Unlimited

17. DISTRIBUTION STATEMENT (of the abstract entered in Block 20, if different from Report)

18. SUPPLEMENTARY NOTES

19. KEY WORDS (Continue on reverse side if necessary and identify by block number)

Extrusion, quench rate, ageing, centerline cracking, void formation, texturing, preferred orientation, hardness, microstructure

2 to 480 K/s

20. ABSTRACT (Continue on reverse side if necessary and identify by block number)

The effects of quench rate, mode of quenching and subsequent ageing treatments on microstructure and properties of a U- wt % Ti alloy have been investigated. Particular emphasis has been placed upon heat treatment of 35mm diameter, γ-extruded, bar. Cooling rates in the range 2 - 480 ks^{-1} were obtained, resulting in a wide spectrum of microstructures ranging from granular α after slow rates of cooling to almost fully martensitic α' after faster cooling. By optimising

Continued ...

20. the rate and mode of quenching the problems of centreline cracking and void formation have been circumvented. Subsequent ageing at 450°C produced hardnesses in excess of 480 Hv_{30} due to precipitation of U_2Ti.

CHARACTERISATION OF URANIUM-¼ % TITANIUM
ALLOYS EXTRUDED FROM THE GAMMA PHASE

FINAL REPORT

by

R.I. Saunderson and G.B. Brook

SUMMARY

High density and tensile properties can be achieved in U-¼ % Ti
by water quenching from the γ phase and subsequently ageing at
lower temperature. These high quench rates have been found to
give rise to centreline cracking and void formation in medium and
large diameter bars (i.e. greater than approximately 20mm diameter).

In the present work the effects of quench rate, mode of quenching
and subsequent ageing treatments on microstructure and properties
of a U-¼ wt % Ti alloy have been investigated. Particular emphasis
has been placed upon heat treatment of 35mm diameter, γ-extruded,
bar.

Cooling rates in the range 2 - 480 Ks^{-1} were obtained, resulting in
a wide spectrum of microstructures ranging from granular α after
slow rates of cooling to almost fully martensitic α' after faster
cooling. By optimising the rate and mode of quenching the problems
of centreline cracking and void formation have been circumvented.

Even at the fastest cooling rates only approximately half to three-
quarters of the available titanium was retained in solution.
Nevertheless, subsequent ageing at $450^{\circ}C$ produced hardnesses in
excess of 480 Hv_{30} due to precipitation of U_2Ti.

Extrusion in the γ phase resulted in a pronounced texture with
(002) perpendicular to the extrusion direction. This preferred

orientation could be eliminated or diminished by reheating into the γ phase. Pronounced texturing was not produced in bars by controlled immersion. However, other work on α-extruded bars has shown that it is possible to induce prominent textures by this method.

CONTENTS

1. INTRODUCTION

Alloys of uranium with molybdenum or titanium have been
developed as possible penetrator materials because of their
high hardness and tensile strength[1]. Of the titanium
containing alloys the composition U-¼% Ti has been selected
for further investigation. The alloy is produced commercially
by casting into 8" and 12" diameter ingots and subsequently
extruding in the γ phase to 1¼" diameter rod. To obtain
optimum properties the extruded rod must be quenched from the
γ phase and aged to peak hardness at temperatures in the region
of 400 - 500°C. Moderately high quench rates are required to
retain sufficient titanium in solution to give a satisfactory
age hardening response. At these quench rates non-uniform
microstructures across the section of bars greater than approx-
imately ¾" diameter give rise to problems of centreline cracking
and void formation.

The aim of the present work has been to obtain a better understanding
of the effects of post extrusion thermal treatment on the micro-
structure and properties of a U-¾wt % Ti alloy. Particular emphasis
has been placed upon the effect of various modes of quenching and
the subsequent ageing of full sized bar specimens, 35mm in diameter.
The possibilities of inducing a transformation texture in these
bars by controlled immersion quenching have also been investigated.

2. TECHNICAL BACKGROUND

i) The Equilibrium Phase Diagram

The uranium-titanium phase diagram has been studied by several workers[2,3,4]. The most comprehensive work is that due to Knapton[5] who reported that above $898^{\circ}C$, γ-uranium and β-titanium form a complete range of solid solutions. An intermediate ε-phase (U_2Ti) forms from γ-uranium at $898^{\circ}C$ and 9.02 wt% Ti. A eutectoid reaction exists at 0.83 wt% Ti and $723^{\circ}C$ by which γ-uranium decomposes to β-uranium and U_2Ti. The β phase transforms to $\alpha + U_2Ti$ at $667^{\circ}C$ and the solubility of titanium in α-uranium is less than 0.18 wt% Ti. The uranium-rich region of the uranium-titanium equilibrium phase diagram due to Knapton[5] is shown in Figure 1. Similar findings have been reported by Udy and Boulger[3,4] but are at variance with Knapton's findings concerning the range of the U_2Ti field, the γ-eutectoid position and the solubility of titanium in α-and β-uranium. The results of Knapton have, however, been confirmed by several workers[6 - 8] and his interpretation of the phase diagram is now widely accepted and has been used throughout the present work.

ii) Nomenclature

The nomenclature used in the present work to denote the various metastable phases and variants was that proposed by Lehmann and Hills[9] in which the symbol α denotes structures which are modifications of orthorhombic α-uranium. A superscript denotes deviations from the orthorhombic structure. The structure resulting from a relative contraction of the 'b' lattice parameter is designated α' while that derived from a relative contraction of the 'b' parameter in conjunction with a change to a monoclinic structure is denoted by α''. Morphological characteristics are denoted by subscripts. The subscripts 'a', 'b' and 'n' are used to denote acicular, banded and nucleation and growth type structures respectively. In a similar manner, superscripts are used to denote crystallographic deviations from the bcc γ-phase. For instance a tetragonal variation of γ would be designated γ°.

3. EXPERIMENTAL DETAILS

Two quenching furnaces have been constructed and used in the present work. The first, a gas quenching furnace, was described in detail in a previous report[10] and comprised of an evacuated column in which the specimen was held and induction heated. Quenching was achieved by opening the vacuum to a reservoir of either argon or helium gas. Quench rates of up to 480 Ks^{-1} were achieved in this way.

The second furnace facilitated liquid quenching of full sized bars under vacuum. The final design is shown diagrammatically in Figure 2. The system was pumped by a 2" oil diffusion pump with liquid nitrogen cold trap. A vacuum of 3×10^{-6} mb was achieved regularly at room temperature. (The pressure was measured at the bottom of the furnace tube). Outgassing for a minimum of 12 hours at $500^{\circ}C$ was necessary in order that the vacuum, during subsequent heating to $780^{\circ}C$, should not deteriorate to worse than 3×10^{-4} mb. On quenching the vacuum deteriorated momentarily to roughly 10^{-1} mb but recovered quickly.

Specimens were of full diameter bar stock, roughly 6" in length. Adsorbed surface layers were removed electrochemically to reduce contamination of the vacuum during heating to temperature and to permit more efficient hydrogen outgassing. Holes were drilled radially in the specimens at 30, 50 and 70mm from the bottom end to accommodate thermocouples. The specimen was secured in a zircaloy-2 collar at one end by means of a ¼" diameter zircaloy-2 pin passing through the specimen and collar. The purpose of the collar was to maintain the specimen centrally in the furnace tube and to ensure that the specimen was positioned correctly for quenching. The vertical position of the specimen in the furnace tube was monitored by means of a 'dummy' specimen outside the furnace.

Ageing of quenched bars was performed in a horizontal ageing furnace at a vacuum of better than 5×10^{-5} mb. The temperature of the specimen was monitored by a Pt/Pt-13Rh thermocouple in contact with the specimen. The temperature of the furnace was controllable to ± $4^{\circ}C$ at $500^{\circ}C$.

4. RESULTS AND COMMENTS

4.1 The As-received Structure

The as-received material was relatively free of inclusions.
A full chemical analysis is shown in Table 1. The principal
impurity is silicon which is most probably concentrated in the
glassy silicate inclusions which are occasionally observed.
The only other impurities present at significant levels are
Mg and Fe. As reported previously, the structure under polarised
light consisted of an irregular α grain structure (Figure 3a).
This bore little resemblance to the etched structure which
consisted of eutectoid $\alpha + U_2Ti$ and residual areas between
the eutectoid regions which had decomposed by nucleation and
growth to a more equiaxed structure. (Figure 3b). The euctectoidal
nature of the microstructure and the titanium distribution are
clearly defined in the scanning electron micrograph and titanium
linescan in Figures 4a and b. The as-received structure was
consistent with that produced by slow cooling from γ. The lack
of correspondence between polarised and etched structures resulted
from the fact that while polarised light revealed the equilibrium
room temperature α structure, the etched structure represented the
titanium distribution established at higher temperatures.

The hardness of the as-received material varied from 336 Hv_{30}
($\pm$ 10 Hv_{30}) at the front end of the extrusion to 314 Hv_{30} at the
trailing end.

4.2 The Effect of Cooling Rate on Microstructure

After cooling from 780°C at between 2 and 10Ks^{-1}, the structure,
viewed under polarised light, consisted of a mixture of equiaxed
and lath-type α (Figure 5a). The orientation of the Widmanstätten-
type α laths changed from one prior γ grain to another and was
thus a function of prior γ orientation. A single phase delineation
of the prior γ boundaries was often observed. After etching
(Figure 5b) the structure consisted of laths of lamellar $\alpha + U_2Ti$

surrounding residual areas which had decomposed to a fine
granular morphology. Very similar structures were observed
after cooling from 880°C indicating that the microstructures
were not significantly affected by holding temperature in the
γ phase. The increase in cooling rate from 2 to 10 Ks^{-1} resulted
in a slight increase in hardness from 311 Hv_{30} to 330 Hv_{30}. This
change may not be significant since it is within the spread of
values obtained from the as-received material.

Increasing the cooling rate to 30 Ks^{-1} produced a structure
which, under polarised light, was comprised of fine, martensitic
α' needles in a very fine granular α matrix (Figure 6). Etching
revealed colonies of α' within the prior γ grain structure. A
differential etching effect was apparent at prior γ grain boundaries.
There was no evidence of a change of titanium content at the
boundaries observed by titanium linescans in the scanning electron
microscope. Under polarised light these regions were comprised
of a fine granual α structure. A significant increase in hardness
to approximately 394 Hv_{30} was obtained.

Further increases in cooling rate to 45, 98 and 170 Ks^{-1} resulted
in progressive increases in the proportion of α' in the structures
and a general coarsening of the martensitic plates until at a cooling
rate of approximately 320 Ks^{-1} (Figure 7) the structure was almost
entirely martensitic. However, the fine granular α persisted at
prior γ boundaries. Similar structures were observed at 480 Ks^{-1}
which was the highest cooling rate achieved in the present work.

The specimens quenched at 98, 320 and 480 Ks^{-1} were too thin to
yield meaningful hardenss measurements. The hardness after quenching
at 170 Ks^{-1} was approximately 414 Hv_{30}($\pm$10 Hv_{30}) which is similar
to that obtained after cooling at 45 Ks^{-1}.

In summary, very slow cooling rates (i.e. 2 Ks^{-1} or less) produced
an equiaxed α structure under polarised light and a lamellar
$\alpha + U_2Ti$ structure after etching. Slightly faster cooling induced
a directionality in the granular α matrix which with further increase

TABLE 1. ANALYSIS OF AS-RECEIVED U-0.75 wt % Ti ALLOY

Element	Concentration (p.p.m. by atoms)
Ti	6,000*
Si	1,000
Mg	100
Fe	30
Ca	10
Al	10
Co	<1
Mn	3
S	10
P	<1
Zn	6
Cu	5
Cr	3
Ni	<3
K	3
U	Base

* This figure is unreliable since mass
spectrometry is not accurate at these
levels of Ti.

in cooling rate gave way to a martensitic α' structure with
fine, granular α at prior γ boundaries.

4.3 Quenching of Full Size Bars

In order to characterise the microstructures obtained by cooling
full size bars, and to relate these to the gas quenched structures,
full size bars (35mm diameter) were quenched by various modes into
oil.

i) Plunge Quenching

The microstructural regions resulting from plunge quenching a
full size bar are shown in Figure 8a. The cooling rate was greatest
at the end of the bar where initial contact was made with the
quenchant. The microstructure in this region (Figure 9a and b),
consisted almost entirely of coarse, martensitic α' with only
occasional non-martensitic regions observed usually at prior γ grain
boundaries. At a distance of approximately 8mm from the end of the
bar the martensitic α' structure persisted. However, a refinement
of the α' lath size and an increase in the amount of fine granular
α at prior γ grain boundaries was observed (Figure 10a). Furthermore,
towards the centre of this region, colonies of fine equiaxed
α were observed which had initiated at prior γ grain boundaries
(Figure 10b). This type of microstructure became more prominent
with increase in distance from the end of the bar. Figures 11a and
b show the structure close to the centre of the bar at 60mm from
the bottom end. The measured cooling rate was approximately 70 Ks^{-1}.
The microstructure consisted of α at prior γ boundaries with
martensitic α' regions within the prior γ grains. Under polarised
light the non-martensitic regions were of two forms; fine equiaxed
granular regions and larger single phase regions such as that marked
'A' in Figure 11a. These two α morphologies may reflect different
modes of transformation from γ. This point will be discussed in
detail later.

Figure 12 shows evidence of star-shaped pores observed at a single
localised region at the centre of the plunge quenched bar , 60mm

from the bottom end. Slight microstructural changes were evident
in the vicinity of the defects. It is possible that these defects
are a type of centreline void formed by quenching. It is also
possible that they were caused by shrinkage porosity not healed
by extrusion of the bar. This was the only observation of such
defects during the present work.

The proportion of non-martensitic α decreased with increased
distance from the centre of the bar. Figure 13 shows the structure
close to the edge of the bar, 60mm from the bottom end. Although
the structure was predominantly martensitic, a fine granular α
delineation of prior γ grain boundaries was evident. With reference
to the gas quenched microstructures, the structure shown in Figure 13
is consistent with a cooling rate of roughly 90 - 100 Ks^{-1}.

With the exception of the porosity defects, the structures observed
at 60mm from the end of the bar were typical of those in the remainder
of the bar.

In general, little variation in hardness of the plunge quenched
bar was observed. The average hardness was 368 Hv_{30} (± 10 Hv_{30})
although a trend towards higher hardnesses e.g. 385 Hv_{30} towards the
centre of the bar was noted. These higher hardnesses at the centre
can be attributed to increased precipitation of U_2Ti during cooling.

ii) End Quenching

A full diameter bar 6" in length, was heated to 780°C and then cooled
by immersion of one end in oil to a depth of 25mm. The rates of
cooling at 700°C at the centreline of the bar, measured at distances
of 30, 50 and 70 mm from the quenched end were 11 Ks^{-1}, 8 Ks^{-1} and
3 Ks^{-1} respectively. The bar could be divided into five micro-
structural regions (Figure 8b). These were:-

1) The high cooling rate at the end of the bar which
made initial contact with the quenchant was reflected
in a coarse, almost fully martensitic α' structure
with fine granular α occasionally observed at prior
γ grain boundaries.

2) Between approximately 2 - 20mm from the quenched end
the martensitic α' structure persisted but the granular
α phase became more predominant at the prior γ boundaries,
(see Figure 14), particularly near the centre of the
bar. At 10mm from the quenched end very fine granular
α was also observed between the α' laths within the
prior γ grains, as in Figure 15.

3) The amount of non-martensitic α increased with distance
from the quenched end of the bar until at 50mm from the
quenched end the structure under polarised light con-
sisted of a low volume fraction of fine α' laths within
a granular α matrix (Figure 16a). Etching did not
highlight the martensitic laths as in previous α'
structures but instead the etched structure adopted a
feathery appearance (Figure 16b and c) more reminiscent
of the lamellar structures produced by slow cooling.

4) At greater distances from the quenched end of the bar the
martensitic structure was replaced by a directional
lath or Widmanstätten-type morphology, which existed
within the coarsened granular α matrix, as shown in
Figure 17a. On etching this structure adopted a feathery
appearance together with regions which were more
obviously eutectoidal, (Figure 17b).

5) Finally, at distances of 75mm and more from the
quenched end the Widmanstätten-type structure gave
way to a fully equiaxed α structure typical of that
after very slow cooling rates in the as-received
material.

The variation of hardness with distance in the end quenched bar is
shown graphically in Figure 18. Up to a distance of 20 - 25mm from
the quenched end the hardness was approximately 370 Hv_{30} ($\pm$ 10 Hv_{30}).
Between 25 and 40mm the hardness increased to approximately 395 Hv_{30}
($\pm$ 10 Hv_{30}) after which it remained almost constant. The drop in
hardness at higher cooling rates is most likely to be due to the
retention of Ti in solution and suppresion of U_2Ti precipitation.

iii) Controlled Quenching at 100 mm/s.

A full diameter bar, 6" in length was heated to 780°C and immersed in oil at a rate of 100 mm/s. The resulting microstructural regions are shown diagrammatically in Figure 8c.

The region immediately adjacent to the end of the bar which made initial contact with the quenchant exhibited an almost fully martensitic α' structure. Prior γ grain boundaries were occasionally delineated by a fine granular α phase. This delineation became more prominent with increased distance from the end of the bar (Figure 19a) although most of the structure remained martensitic (Figure 19b). Finer laths within the coarse martensitic α' laths could be resolved at higher magnifications after etching, as in Figure 20. At a distance of roughly 30 - 35mm from the bottom end the α' lath size became more refined and more extensive regions of granular α were observed at prior γ grain boundaries. A typical structure is shown in Figure 21. At 50mm from the bottom end extensive colonies of granular α were observed (Figure 22). Martensitic areas persisted between the α colonies. This microstructure was typical of that in the remainder of the bar where the measured cooling rate was approximately 65 Ks^{-1}.

The variation in hardness with distance from the bottom of the bar is shown graphically in Figure 23. The hardness increased slightly from 340 to 370 Hv_{30} (± 10 Hv_{30}) over the first 40mm from the end of the bar. Thereafter it remained almost constant at 370 - 380 Hv_{30} with increased distance from the end of the bar. This trend is similar to but less pronounced than that in the end quenched bar where the hardnesses were generally 20 - 30 Hv_{30} higher. This difference can be ascribed to the higher cooling rate in the controlled quenched bar and hence less precipitation of U_2Ti during the quench.

iv) Controlled Quenching at 10 mm/s.

The microstructural regions resulting from controlled quenching at an immersion rate of 10 mm/s are shown in Figure 8d. Microstructurally,

the bar was very similar to that quenched by immersion at 100mm/s
except that the slower immersion rate (and hence slower cooling
rate) promoted the formation of non-martensitic α. This manifested
itself in a shift of all the microstructural zones towards the bottom
end of the bar. Figures 24a and b are typical of the structure
observed in the greater portion of the bar which was comprised of
martensitic α' within prior γ grains and fine granular α in colonies
and delineating prior γ grain boundaries. It is interesting to note
that compared with the bar immersed at 100 mm/s, the rate of immersion
of the present specimen was reduced by an order of magnitude but the
cooling rate measured at similar points in the bars fell from approx-
imately 65 Ks^{-1} to 50 Ks^{-1}.

The hardness variation in the bar immersed at 10 mm/s showed a
similar trend to that in the bar immersed at the faster rate. The
hardness rose from a value of approximately 350 Hv_{30} to the end of
the bar and remained almost constant at 370 Hv_{30} at distances greater
than 25mm from the end.

4.4 The Effect of Ageing

Previous work[11,12] has indicated that peak hardness in the present
alloy can be achieved by ageing for approximately 3 hours at 450°C.
The end quenched bar specimen was therefore given this ageing treatment
in order to determine the effect of ageing on the full range of
microstructures. A second bar, controlled quenched at 100mm/s, was
also aged with a view to determining the hardening response obtainable
in bars oil quenched after γ extrusion.

i) Ageing of End Quenched Bars

Ageing of the end quenched bar for 3 hours at 450°C had little
discernible effect upon the optical microstructure. As in the unaged
bar, the structure, up to approximately 50mm from the quenched end,
consisted of a mixture of martensitic α' and fine granular α ; the
latter being usually associated with prior γ grain boundaries.
Figure 25 shows a typical microstructure. At greater distances from
the end of the bar the microstructure adopted a Widmanstätten

appearance (Figure 26) which, with increased distance, gave way
to an equiaxed granular α structure.

The variation in hardness with distance in the bar after ageing
is shown in Figure 18 where it is compared with the unaged hardness.
Hardnesses in the region of 460 - 490 Hv_{30} were achieved in the
first 20 - 30mm of the specimen. At greater distances from the
quenched end the hardness dropped to approximately 390 - 400 Hv_{30}.
By comparison with the unaged hardness it is seen that at a distance
of 30mm and over,little or no hardening was achieved by ageing at
$450^{\circ}C$. However, in regions of the specimen where the quench rate
was sufficiently high to retain appreciable amounts of titanium in
solution (i.e. at less than 30mm from the quenched end), an increase
in hardness of approximately 100 Hv_{30} was achieved. It is concluded
that while only comparatively low hardnesses can be achieved by the
retention of titanium in solution, the hardness can be considerably
increased by the precipitation of titanium in the form of U_2Ti.

ii) Ageing of Bar Controlled Quenched at 100 mm/s.

Ageing of the end quenched bar indicated that a sufficiently high
cooling rate achieved thoughout a bar would result in a good hardening
response on subsequent ageing. The bar quenched by immersion in oil
at 100 mm/s was therefore aged for 3 hours at $450^{\circ}C$. By comparison
with the unaged bar, little change in microstructure resulted from
ageing although some evidence suggested that the granular α regions
at prior γ grain boundaries were slightly more extensive after ageing.
This was difficult to quantify.

The variation of hardness with distance in the bar after ageing
is shown in Figure 23. Close to the end of the bar where the initial
quench rate was highest ageing resulted in an increase in hardness
from 340 to 520 Hv_{30}. In most of the bar, where the cooling rate had
stabilised at approximately 65 Ks^{-1}, (measured on the centreline of
the bar) ageing produced a hardness of between 470 and 480 Hv_{30} which
represented an increase of approximately 100 Hv_{30} over the as-quenched
material.

TABLE 2 : RESULTS OF X-RAY EXAMINATION

HEAT TREATMENT	b (Å)	COMPOSITION (At.% Ti)	TEXTURE COEFFICIENTS OF FIVE MOST PROMINENT PLANES					COMMENT
As received	5.858	1.8** / 0.6+	(002) 3.2	(021) 2.8	(111) 2.4	(110) 0.6	(040) 0.2	Sharp U_2Ti peaks. No α_1/α_2 resolution.
Radiation cooled from 780°C @ 2 Ks^{-1}	5.857	1.9 / 0.7	(002) 0.8	(021) 1.3	(111) 0.7	(200) 0.9	(040) 0.9	Sharp U_2Ti peaks. Partial α_1/α_2 resolution.
Radiation cooled from 880°C @ 2 Ks^{-1}	5.857	1.9 / 0.7	(002) 1.5	(021) 1.4	(111) 1.3	(200) 0.9	(110) 0.9	As above
Gas quenched from 780°C @ 100-300 Ks^{-1}	5.846	2.8 / 1.8	(002) 0.7	(021) 0.6	(111) 0.7	(130) 2.1	(113) 2.4	Very weak U_2Ti peaks. No α_1/α_2 resolution.
Bar, plunge quenched from 780°C	5.850	2.4 / 1.3	(002) 2.0	(021) 1.9	(111) 1.2	(130) 0.9	(042) 2.2	Very weak U_2Ti peaks. No α_1/α_2 resolution. Examined 60mm from bottom end. (~70 Ks^{-1})
Bar, end quenched from 780°C	5.854	2.1 / 1.0	(002) 2.1	(021) 1.5	(111) 1.3	(130) 0.9	(042) 1.7	Weak U_2Ti peaks. No α_1/α_2 resolution. Examined 60mm from end. (~6 Ks^{-1})
Bar, control quenched from 780°C Immersion rate 100 mm/s	5.846	2.8 / 1.8	(002) 1.3	(021) 2.0	(111) 1.5	(130) 1.6	(042) 1.5	Very weak U_2Ti peaks. No α_1/α_2 resolution. Examined 15mm from bottom end. (~80 Ks^{-1})
Bar, control quenched from 780°C Immersion rate 10 mm/s	5.851	2.3 / 1.2	(002) 0.9	(021) 1.1	(111) 1.5	(130) 1.3	(042) 0.9	As above

* Compositions obtained using lattice parameter/composition curves due to Anagnostidis et al (13)
** " " " Douglass (14)
\+ " " "

NOTE : All specimens were examined with surfaces perpendicular to extrusion direction.

4.5 X-Ray Diffraction Studies

Selected specimens were examined by X-ray diffraction in order
to determine:-

a) preferred orientation

and b) amount of titanium in solid solution by
'b' lattice parameter determination.

The preferred orientation of samples was investigated by
determining texture coefficients (TC) for diffraction peaks
using the expression:

$$TC = \left({}^I\!/I_o\right)_{hk\ell} \Big/ \frac{1}{n}\Sigma\left({}^I\!/I_o\right)_{hk\ell}$$

in which I is the observed height of the hkℓ peak

I_o is the corresponding intensity for a random sample
and n is the number of diffraction peaks employed
in the analysis.

A texture coefficient is proportional to the volume amount of
material which is oriented with an {hkℓ} plane parallel to the
surface of the sample. The sample surfaces examined were
perpendicular to the long direction of the bar. Hence the
texture coefficient so obtained revealed the way in which the
α was orientated relative to a plane perpendicular to the extrusion
direction, i.e. the orientation of α along the extrusion direction.

The results of the X-ray examinations are shown in Table 2. A
pronounced (002) texture was observed in the as-received material
which had been γ extruded. Subsequent reheating into γ and cooling
at various rates between 2 Ks^{-1} and 300 Ks^{-1}, destroyed or reduced
this (002) texture. No strongly preferred orientation was observed
in any of the specimens examined. Slow cooling from 780°C at 2 Ks^{-1}
produced an almost random structure while cooling at the same rate
from 880°C produced a slightly more prominent (002) texture

although this was still relatively weak. Increased cooling rate
to between 100 and 300 Ks^{-1} produced prominent (130) and (113)
textures. Quenching of bar specimens did not produce strongly
pronounced textures although (021) and/or (002) were prominent
in these specimens.

The 'b' lattice parameter of uranium is the most sensitive to
solute content and decreases with increased titanium in solution.
The accepted 'b' lattice parameter for pure uranium is 5.868Å
while that of U-¼ wt % Ti, with all the titanium in solution, is
either 5.820Å or 5.828Å, depending upon whether the data of
Anagnostidis et al[13] or Douglass[14] respectively is used. The
data from these two sources are plotted for comparison in Figure 27.
The reason for the discrepancy in the curves is not obvious.
Anagnostidis et al heat treated <2mm thick slices in vacuum followed
by water quenching after back-filling the system with argon.
Douglass used encapsulated wafers which were quenched into water.
Neither quench rate nor specimen thickness is known but no evidence
of U_2Ti formation was detected. It is known that at high quench
rates and a given solute content the 'b' lattice parameter can
increase with increasing quench rate. Hence the discrepancy may
be due to a difference in quench rates.

The discrepancy could also be due to differing effective solute
contents e.g. some titanium could have been removed from solution
as insoluble TiC by reaction with carbon impurities. Unfortunately,
accurate chemical analyses are not available and in the absence
of more detail of experimental methods is is impossible to resolve
the discrepancies between the two sets of data.

In the present work the level of titanium retained in solution
was lowest in the as-received and slow cooled materials. The
presence of sharp U_2Ti diffractions from these specimens confirmed
that titanium had precipitated from solution during the slow cool
from γ. At faster cooling rates only very weak U_2Ti diffractions
were observed and the level of titanium retained in solution was
generally higher. The general absence of α_1/α_2 peak resolution
can be ascribed to lattice strains resulting from precipitation
of U_2Ti, quenching strains (i.e. transformation strains), or
possibly titanium retained in solution.

5. GENERAL DISCUSSION

It has been shown that the room temperature microstructure of
U-¼% Ti is a sensitive function of cooling rate from the γ phase.
From the gas quenching experiments it has been determined that
the significant quench rates are:-

a) <2 Ks^{-1}. At the slowest rate of cooling from
γ the structure consists crystallographically of
equiaxed granular α, as revealed by polarised
light. Etching, which reveals the 'chemical
structure', produces a eutectoidal microstructure
reflecting the titanium distribution established
at higher temperatures.

b) 2 - 30 Ks^{-1}. Cooling rates between 2 and 10 Ks^{-1}
result in structures comprised of oriented laths of
Widmanstätten-like α in an equiaxed granular α matrix.
The directionality of the Widmanstätten-type structure
becomes increasingly pronounced as the cooling rate
is increased to approximately 30 Ks^{-1}.

c) 30 Ks^{-1} upwards. At cooling rates in the region of
30 Ks^{-1} martensitic α' needles are observed within a
granular α matrix. As the cooling rate is increased
the martensitic structure becomes increasingly pre-
dominant until at quench rates in excess of ~100 Ks^{-1}
the structure is almost fully martensitic. However,
a fine granular α delineation of the prior γ grain
boundaries persists even at cooling rates in the
region of 480 Ks^{-1}. This fine granular α phase is
assumed to have been formed by nucleation and growth
during the quench.

Neither metallography or X-ray examination revealed any evidence of
β phase retention at room temperature, regardless of cooling rate.
The rôle of β phase in the γ → α decomposition must therefore be
deduced by reference to room temperature microstructures. At very
slow cooling rates β formed initially from γ by nucleation and growth.

Depression of the $\gamma \rightarrow \beta + U_2Ti$ eutectoid temperature resulted in a higher proportion of β in the structure than would be expected under equilibrium cooling conditions. The structure thus consisted of areas of β surrounding residual γ regions which subsequently transformed to $\beta + U_2Ti$. On further cooling α nucleated from β and grew to form the roughly equiaxed structure observed under polarised light.

A similar sequence of precipitation occurred at slightly faster cooling rates except that a Widmanstätten-type lath precipitation of β from γ was induced. Furthermore, the residual γ regions may have transformed directly from γ to $\alpha + U_2Ti$ producing a granular or fine lamellar structure.

At higher cooling rates (i.e. in excess of 30 Ks^{-1}) martensitic α' needles were observed. This indicated that transformation from α to β was suppressed to below the M_s temperature of 615°C, determined by Eckelmeyer and Zanner[15], and the fine granular α matrix was formed directly from γ. On etching this matrix appeared featureless, in contrast to the eutectoidal appearance associated with slower cooled microstructures. This was indicative of the fact that at higher quench rates a higher proportion of titanium was retained in solution where its distribution was approximately uniform. This argument is supported by the results of the X-ray examination which confirmed that a large proportion of titanium remained in solution after the faster quenches. For instance, after quenching at approximately 100 Ks^{-1} or more, approximately $\frac{1}{2}$ - $\frac{1}{4}$ of the available titanium was retained in solution. (Note: 0.75 wt % Ti $\cong$ 4 at % Ti).

The above levels of titanium retention would result in a considerable increase in mechanical properties if the titanium were precipitated as U_2Ti by low temperature ageing. In Appendix A it has been assumed that 2 at % titanium is precipitated as U_2Ti. It is shown that this would result in a precipitate volume fraction of roughly 0.05. Assuming that this precipitate is uniformly distributed throughout the matrix in the form of 100Å diameter spheres, it is shown that the average distance of closest approach of the particles is

approximately 20$\overset{\circ}{A}$. If the particles were coarsened to 500$\overset{\circ}{A}$ the
average distance between particles would be approximately 80$\overset{\circ}{A}$. This
would be expected to result in significant levels of strengthening.

The above predictions are borne out by the results of ageing
treatments on end quenched and controlled quenched bars. With
reference to the end quenched bar, hardness measurements indicated
that only a comparatively low level of strengthening could be
achieved by retaining titanium in solution. However, in regions
of the bar where a lower quench rate had resulted in precipitation
of U_2Ti during the quench, a slightly higher hardness was achieved.
After ageing this situation was reversed. The highest hardness was
obtained in regions of the bar which had retained most titanium in
solution during quenching, (see Figure 18). Very little age
hardening occurred in regions where U_2Ti had precipitated during
the quench. However, X-ray examination of the slower cooled regions
of the end quenched bar indicated that between 1 - 2 at % titanium
remained in solution after quenching, (see Table 2). This level of
titanium should produce significant levels of precipitation hardening.
The fact that no precipitation hardening was obtained in the slower
cooled regions of the bar (Figure 18) suggests that exsolution of the
titanium during ageing promoted growth or overageing of the existing
precipitates rather than the nucleation of a fine distribution of
U_2Ti.

The X-ray results indicated that between 2 and 3 at % titanium was
retained in solution in the bar quenched at an immersion rate of
100 mm/s. Ageing resulted in a general increase in hardness of
typically 120 - 130 Vickers hardness points to approximately 475 Hv_{30},
although larger increases were observed near the end of the bar where
the initial cooling rate was greatest. The significance of these
results is two-fold. Firstly, they confirm that hardnesses in
excess of 480 Hv_{30} are obtainable in these bars. A series of isothermal
and isochronal experiments should now be carried out on similarly
quenched bars in order to determine the optimum ageing treatment.
Secondly, they show that full diameter bars can be quenched at a
sufficiently high rate to give a good hardening response on

subsequent ageing, yet without inducing quench cracking or centreline void formation. The negative volume change associated with the $\gamma \rightarrow \alpha$ transformation in U-Ti can produce sufficiently high stresses in quenched rods to result in the above types of defects[12,16]. For example, after water quenching a bar $1\frac{3}{8}$" diameter x 4" long from $800^{\circ}C$, Ammons[12] has measured residual tensile stresses of 110 and 85 ksi in the longitudinal and tangential directions respectively. Anderson[16] has also observed large centreline voids in $1\frac{1}{2}$" diameter U-$\frac{3}{4}$ Ti bar similarly quenched.

In the present work the only evidence of centreline defects observed were pores at a single position in the plunge quenched bar. These pores were not observed in a region of the bar which had undergone the highest rate of cooling and it is considered more likely that they resulted from shrinkage during or immediately after γ phase extrusion rather than from quenching effects. These defects apart, no evidence of quench-induced centreline defects was observed in any of the specimens. This can be ascribed to the moderate quench rates obtained by oil quenching rather than water quenching.

The γ extruded, as-recieved material exhibited a prominent texture with (002) perpendicular to the extrusion direction. (021) and (111) textures were also prominent. These textures could be partially destroyed by reheating into the γ field followed by quenching at up to approximately 300 Ks^{-1} which produced almost random orientation. Pronounced textures were not induced by controlled immersion at 100 mm/s or 10 mm/s. This is somewhat surprising since in other work an α-extruded U-$\frac{3}{4}$ Ti[17] in the form of 30mm diameter bar the (002) extrusion texture was replaced by a prominent (200) transformation texture after controlled immersion. Further effort is required to produce more prominent transformation textures in the present bars. The desirability of inducing certain textures in uranium and its alloys arises from the fact that at room temperature there exists only one easy slip system[18] i.e. (010) $[100]$, and it has been found possible to achieve significant levels of texture strengthening. For instance,

while the Young's modulus of nontextured, polycrystalline, pure
α-uranium is 29×10^{-6} lbf.in^{-2} at room temperature it can be
varied between 21×10^{-6} and 41×10^{-6} lbf.in^{-2} by suitable
texturing[19,20].

6.   CONCLUSIONS

The following conclusions are drawn from the present work:-

   i) The as-received material has a roughly equiaxed, granular
      α structure with U_2Ti distributed as particles in
      one phase of a fine lamellar structure. The structure is
      consistent with that expected in a material slow cooled
      from the γ phase subsequent to final processing.

      The material has a relatively low inclusion content,
      most of which were in the form of glassy silicates.

  ii) Cooling rates from the γ phase have been varied between
      2 and 480 Ks^{-1}. This resulted in microstructures
      ranging from granular α after slow cooling to almost
      fully martensitic α' at the higher cooling rates. The
      fine grained α produced by the slowest cooling rates
      bore little relationship to the eutectoid-like structure
      found on etching. At slightly increased rates of cooling
      oriented laths of α (probably derived from the β phase)
      existed within prior γ grains, the remainder of which had
      transformed to a roughly equiaxed α structure. At quenching
      rates in excess of approximately 30 Ks^{-1} increasingly
      greater proportions of martensitic α' were observed in a
      granular α matrix.

 iii) The general absence of centreline cracking or void
      formation is attributed to the moderate quench rates which
      are, nevertheless, sufficiently high to retain approximately
      half of the available titanium in solution.

  iv) Ageing resulted in marked increases in hardness to approximately
      480 Hv_{30} generally, with higher values (up to 520 Hv_{30}) in
      regions where the initial quench rate was highest.

   v) A pronounced (002) texture existed in the as-received
      material. This persisted, but was much less pronounced, after
      reheating into the γ phase field and cooling at any rate.

Strong transformation textures were not produced by controlled immersion quenching at rates of immersion of 10 or 100 mm/s. However, (002), (021) and (111) textures were generally prominent in these specimens. Furthermore, other work on a similar alloy extruded in the α phase has shown that more pronounced textures can be induced by controlled quenching at certain rates of immersion.

7. REFERENCES

1. Sandstrom, D.J. In "Proc of High Density Alloy Penetrator
    Materials Conf.", AMMRC., Watertown, USA, 1977, P 419.

2. Buzzard, R.W., Liss, R.B., Fickle, D.P.., J.Res.Nat.Bur.Stand.,
    50, (4), 209, 1953.

3. Udy, M.C., Boulger, F.W., Trans. A.I.M.E., 200, 207 & 1317, 1954.

4. Udy, M.C., Boulger, F.W., Report BMI 774, U.S. Atomic Energy
    Commission Publicn. 1952.

5. Knapton, A.G., J.I.M., 83, 497, 1954.

6. Adda, Y., Beyeler, M., Kirianendo, A., Maurice, R.,
    Mem.Sci.Rev.Met. 58, 716, 1961.

7. Howlett, B.W., Knapton, A.G., In "Proc 2nd UN Int.Conf. on
    Peaceful Uses of Atomic Energy", 6, Geneva, 1958, p 104.

8. Linard, M., U.S. Atomic Energy Commission Report ORNO-tr-2579,
    July 1971.

9. Lehmann, Mme. J., Hills, R.F., J.Nuc.Mat., 2, (3), 261, 1960.

10. Saunderson, R.I., Brook, G.B., F.R.I. Report R812/3. This
    Contract, August 1980.

11. Eckelmeyer, K.H., "Ageing Phenomena in Dilute Uranium Alloys"
    in "Physical Metallurgy of Uranium Alloys", ed. Burke, J.J.
    et al., Brook Hill, 1976, P463.

12. Ammons, A.M., "Precipitation Hardening in Uranium Rich
    Uranium Alloys". IBID, P511.

13. Anagnostidis, M., Bauschwitz, R., Colombie, M., Mem.Sci.
    Rev.Met., 63, 163, 1966.

14. Douglass, D.L., Trans. A.S.M. 53, 307, 1961.

15. Eckelmeyer, K.H., Zanner, R.J., J. Nuc.Mat., <u>67</u>. 33, 1977.

16. Anderson, R.C., Unpublished Work, Cited as Ref. 25 in Ref. 12.

17. Saunderson, R.I., Brook, G.B., Unpublished Work, Fulmer
    Research Institute, 1981.

18. Yoo, M.H., J. Nuc.Mat., <u>26</u>, 307, 1968.

19. Armstrong, P.E., Eash, D.T., Hockett, J.E., J. Nuc.Mat.,
    <u>45</u>, 211, 1972.

20. Fisher, E.S., J. Nuc.Mat., <u>18</u>, 39. 1966.

21. Pearson, W.B., "Handbook of Lattice Spacings and Structures
    of Metals", Vol. 1, p 874, Permagon Press, 1958.

22. Hertz, P., Math.Ann., <u>67</u>, 387, 1909.

23. Chandrasekhar, S., Rev.Mod.Phys., <u>15</u>, 1943.

CALCULATION OF NUMBER AND DISPERSION OF U_2Ti PARTICLES CORRESPONDING TO PRECIPITATION OF 2at%Ti FROM URANIUM

It is assumed that 2at%Ti is precipitated from solution in the form of stoichiometric U_2Ti.

Parameters of U_2Ti unit cell [21]

Hexagonal $a = 4.828\overset{\circ}{A}$ $c = 2.847\overset{\circ}{A}$

Volume of unit cell $= \sqrt{3}/2\ a^2 c$

$$= 0.866(4.828)^2 \times 2.847 \times 10^{-24}\ cm^3$$

Number of U_2Ti unit cells

For 2at%Ti, number of unit cells =

$$\frac{2\rho N}{100 \times AT.\ WT.\ U}\ cells\ cm^{-3}$$

where N = Avagadro's number

ρ = density of uranium = 19.05 gm cm^{-3}

Hence,

$$number\ of\ cells = \frac{2 \times 19.05 \times 6.0235 \times 10^{23}}{100 \times 238.03}$$

$$= \frac{3.81 \times 6.0235 \times 10^{24}}{2.3803 \times 10^4}\ cells\ cm^{-3}$$

Total volume of U_2Ti precipitate corresponding to 2at%Ti

Total volume of cells = Volume/cell x Number of cells

$$= 0.866(4.828)^2 \times 2.847 \times 10^{-24} \times \frac{3.81 \times 6.0235 \times 10^{24}}{2.3803 \times 10^4}$$

$$= 5.541 \times 10^{-2}\ cm^3$$

Now assume that the above volume of U_2Ti precipitate is uniformly distributed in the form of spherical particles $100\overset{\circ}{A}$ in diameter.

Volume of $100\overset{\circ}{A}$ diameter sphere $= {}^{4}/_{3}\ \pi\ r^3$

$$= \pi/6 \times 10^{-18}\ cm^3$$

Number of precipitates/cm^3 = N_v = $\dfrac{Total\ volume\ to\ be\ precipitated}{Volume/particle}$

$$= 10.6 \times 10^{16} \simeq 10^{17}\ cm^{-3}$$

Average distance between precipitate centres

Following Hertz [22] and Chandrasekhar [23], the average distance, $\bar{\lambda}$, between randomly distributed particle centres in a volume, V, is given by:

$$\bar{\lambda}_v = 0.554 \; N_v^{-1/3}$$

$$= 0.177 \times 10^{-5} \, cm$$

$$\simeq 120 \mathring{A}$$

Hence for $100\mathring{A}$ diameter speheres the average distance of closest approach is $20\mathring{A}$.

If the sphere diameter is increased to $500\mathring{A}$ the above calculation can be repeated to predict an average distance of closest approach of approximately $80\mathring{A}$.
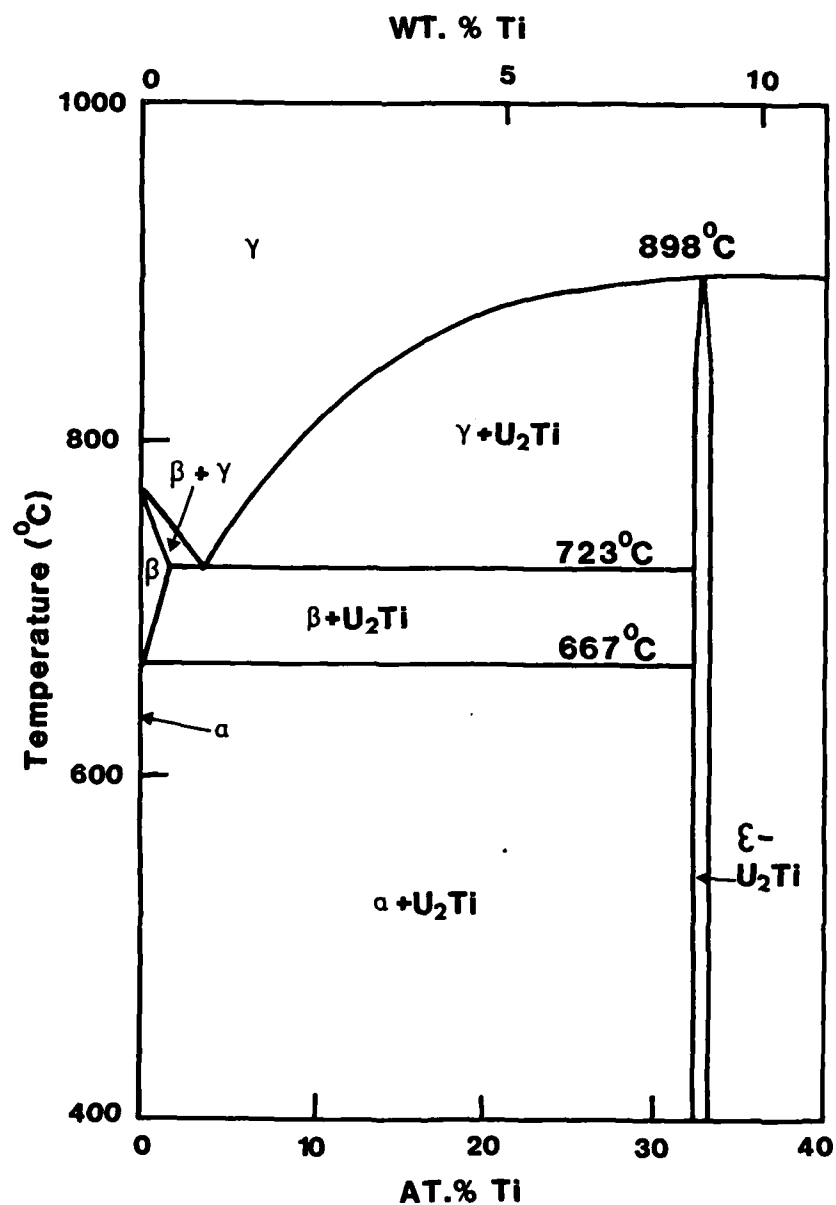
Figure 1 The uranium-rich portion of the uranium- titanium phase diagram, after Knapton(5)

Note: 3/4 WT. % Ti ≃ 4 AT. % Ti

Thermocouple feedthroughs

Pt/Pt-13Rh Thermocouple leads

Reversible D.C. motor

H₂O OUT

Water cooling collar

H₂O IN

Tantalum wire

Zircaloy-2 collar

Specimen

Furnace

Cooling coils

Removable stop flange

Quenching tank

Liquid nitrogen cold trapped diffusion pump
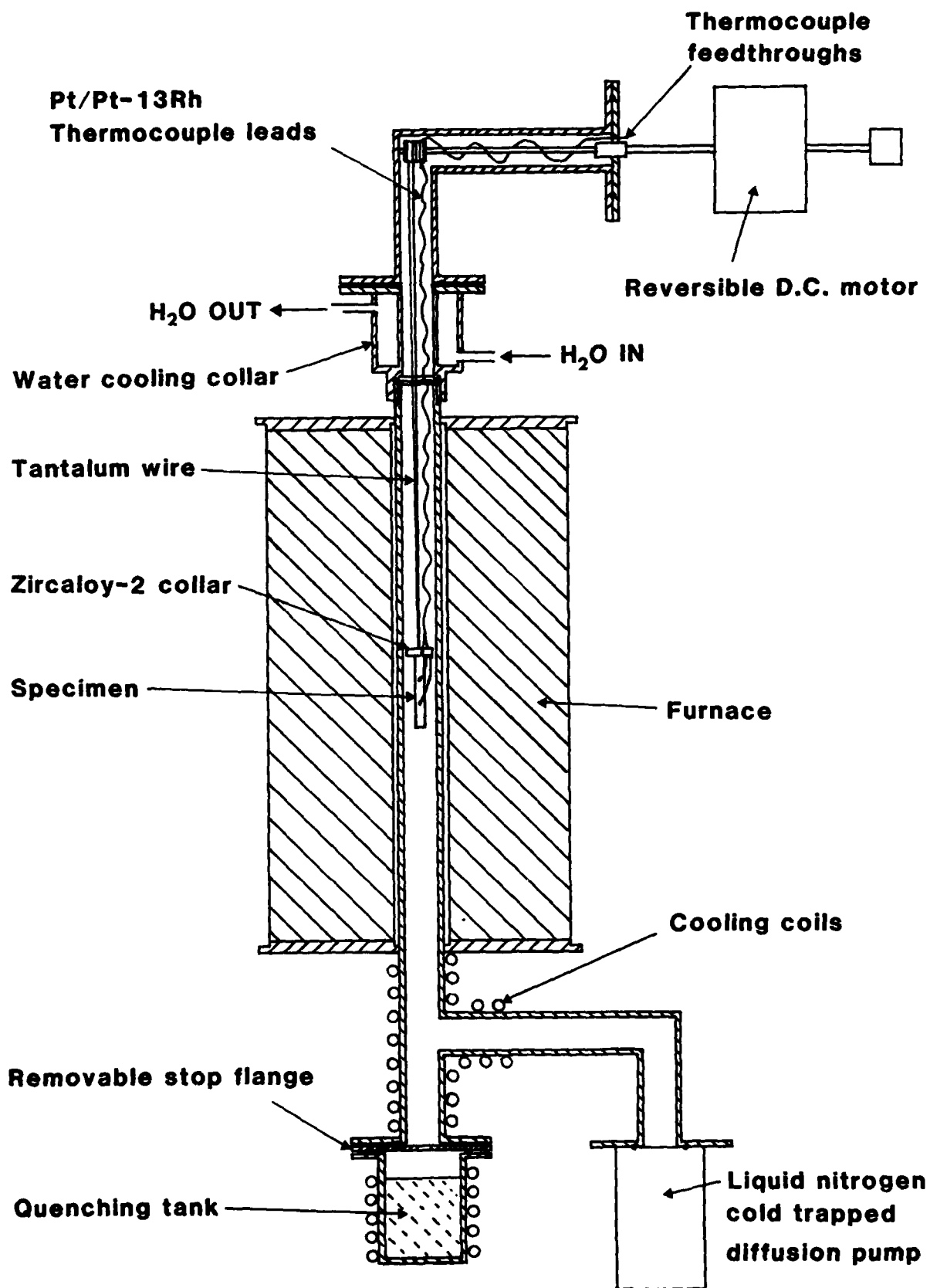
Figure 2 . Diagram of vertical quenching furnace
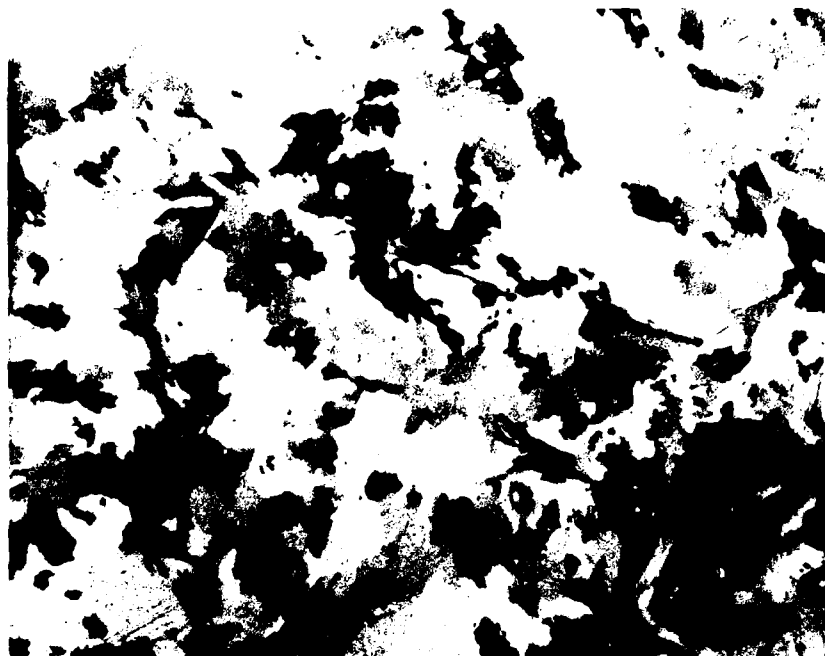
Figure 3a. CROSSED POLARS x 150

F4680

Figure 3b. ETCHED (BRIGHT FIELD) x 150

F4681

Figure 3. Microstructure of as-received material.
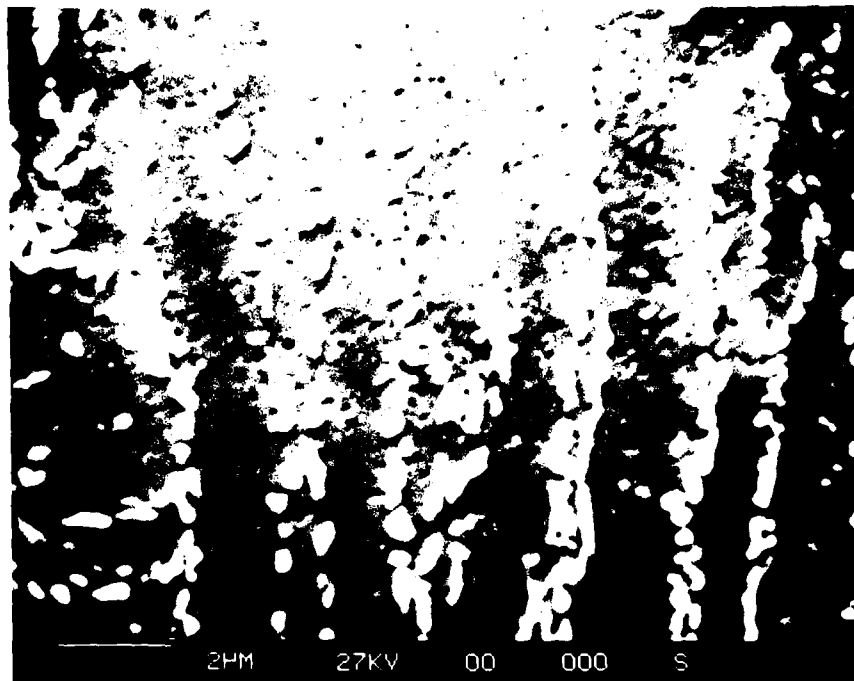
Figure 4a.   PO304

Figure 4b.   PO305

Figure 4.   Scanning electron micrograph (Figure 4a)
             and linescan for titanium (Figure 4b) from
             as-received material.

R812/4

Figure 5a.   CROSSED POLARS   x 150
   F3797
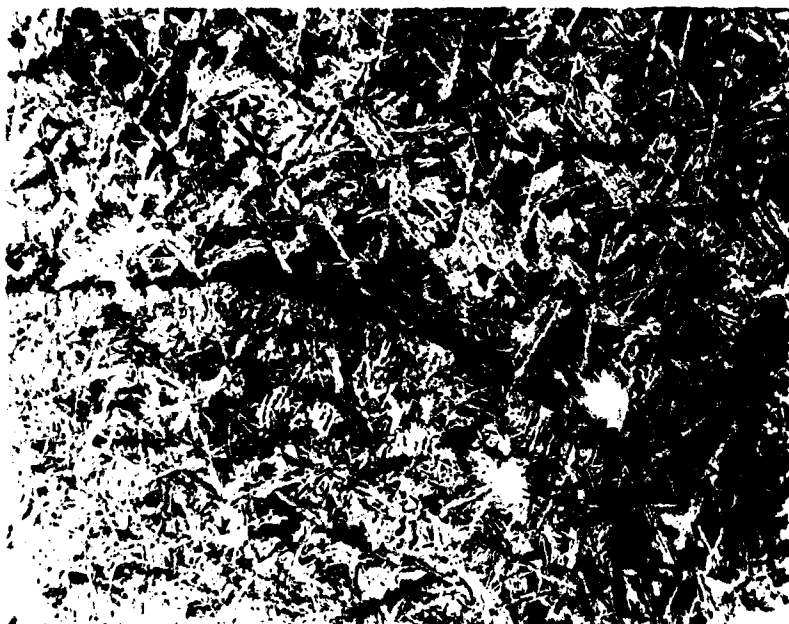
Figure 5b.   ETCHED (BRIGHT FIELD)   x 150
                                                          F3798

Figure 5.   Showing the microstructure after cooling at $10KS^{-1}$.
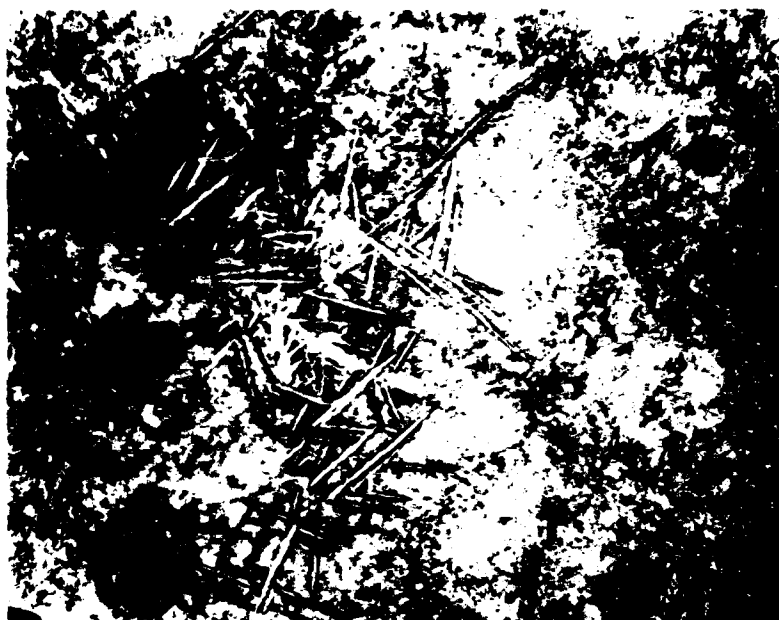
Figure 6.   Showing microstructure after cooling   x 150
             at 30 Ks^{-1}. ETCHED AND CROSSED POLARS   F3911
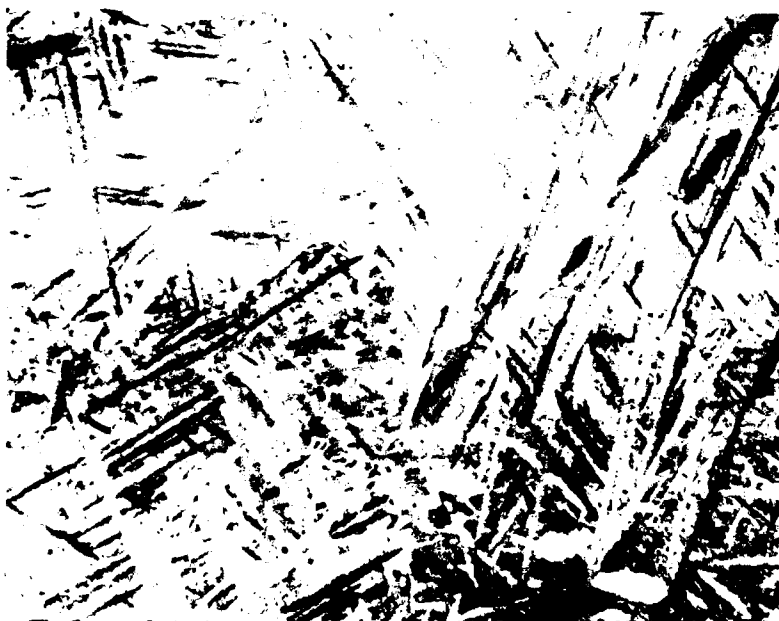
Figure 7.   Showing microstructure after cooling at   x 150
             320 Ks^{-1}. CROSSED POLARS   R3761
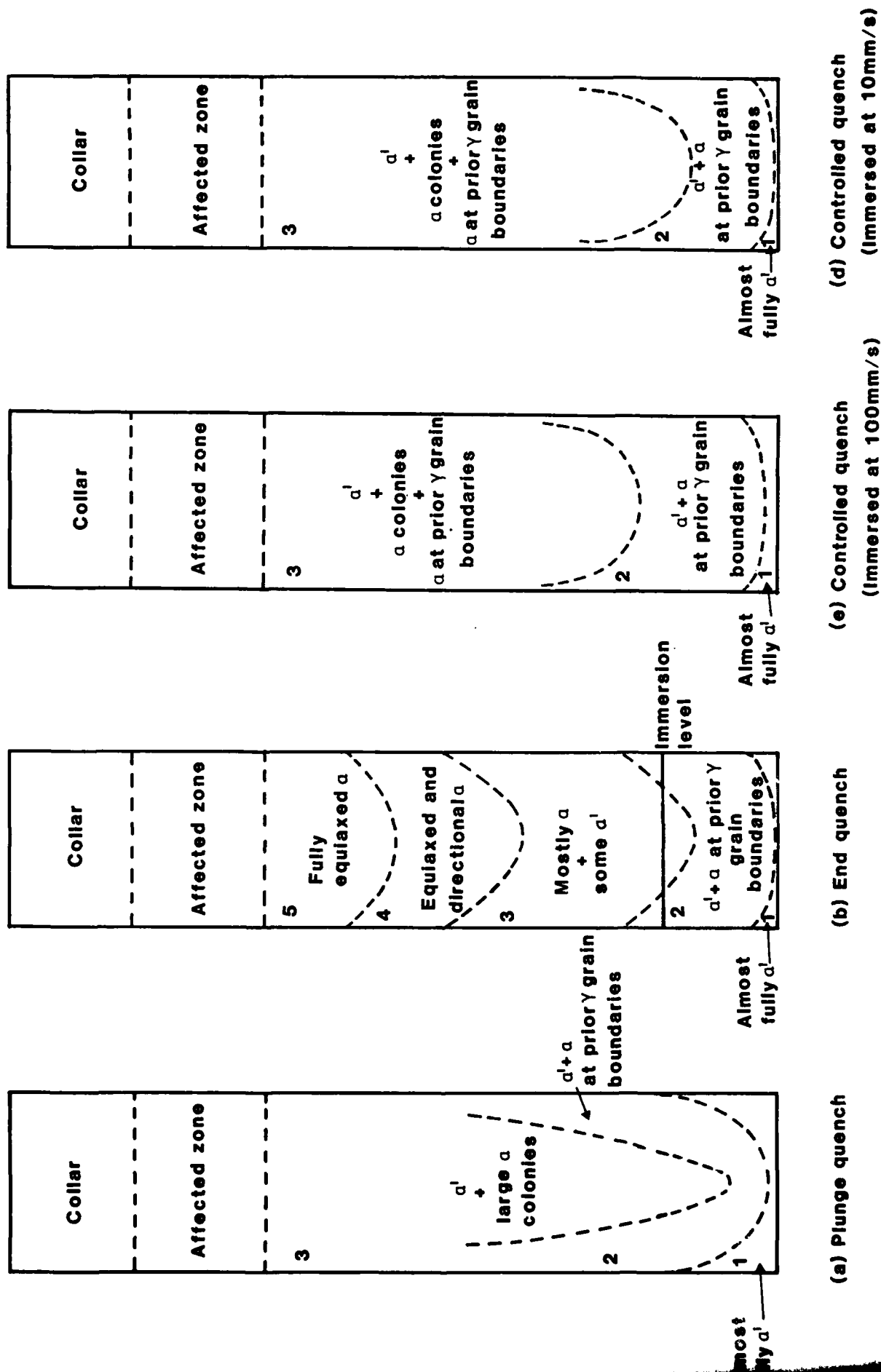
R812/4

Figure 8 Microstructual regions in quenched bars

Figure 9a.   CROSSED POLARS   x 150
                                                 F4654
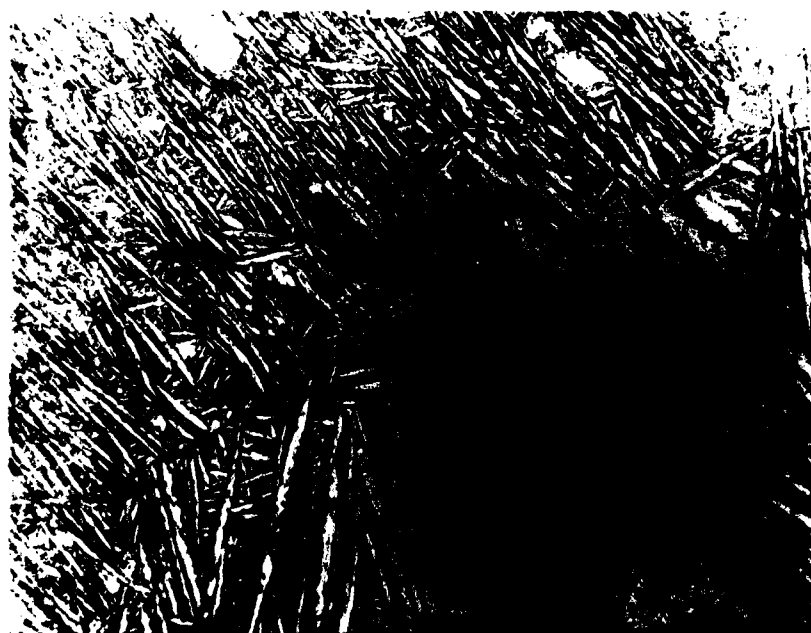
Figure 9b.   ETCHED (BRIGHT FIELD)   x 150
                                                 F4658

Figure 9.   Showing general microstructure 2mm
             from end of of plunge quenched bar.   R812/4
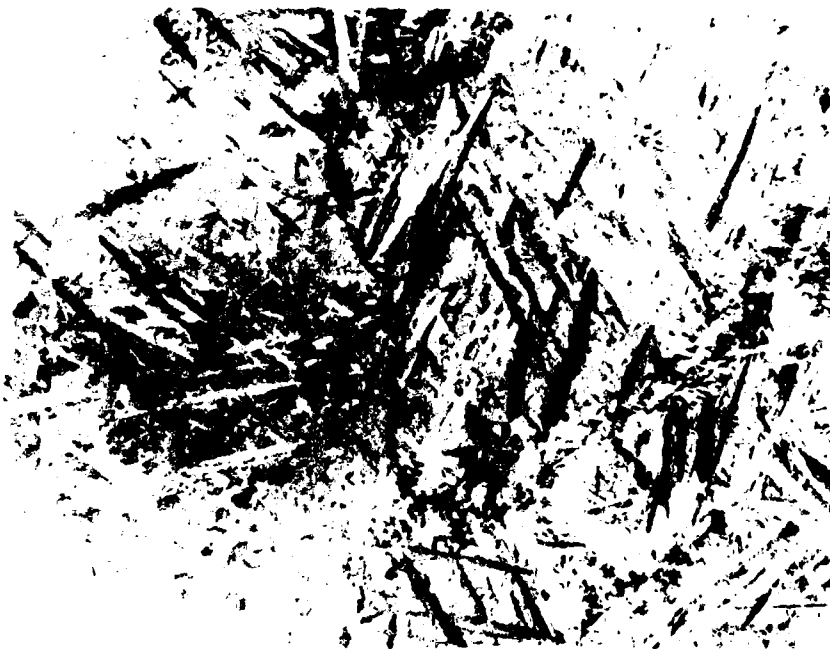
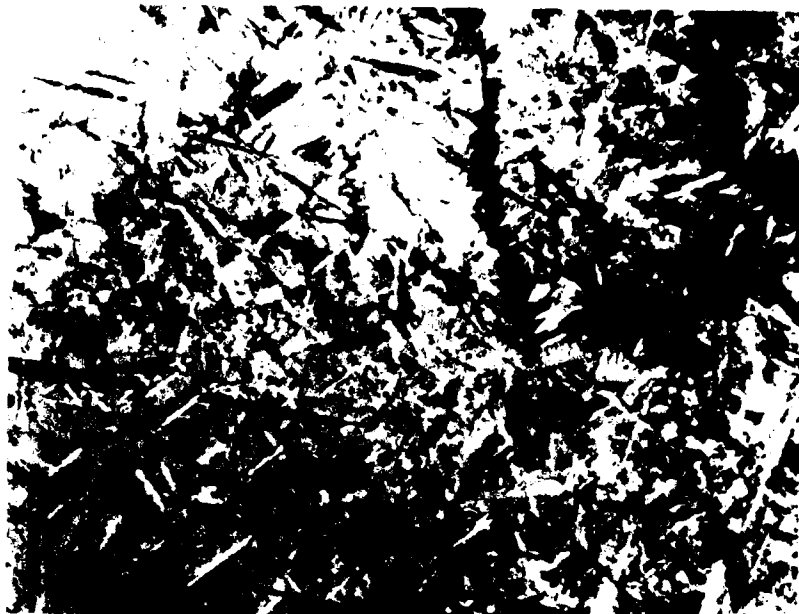Figure 10a.   CROSSED POLARS   x 150
                                                       F4657
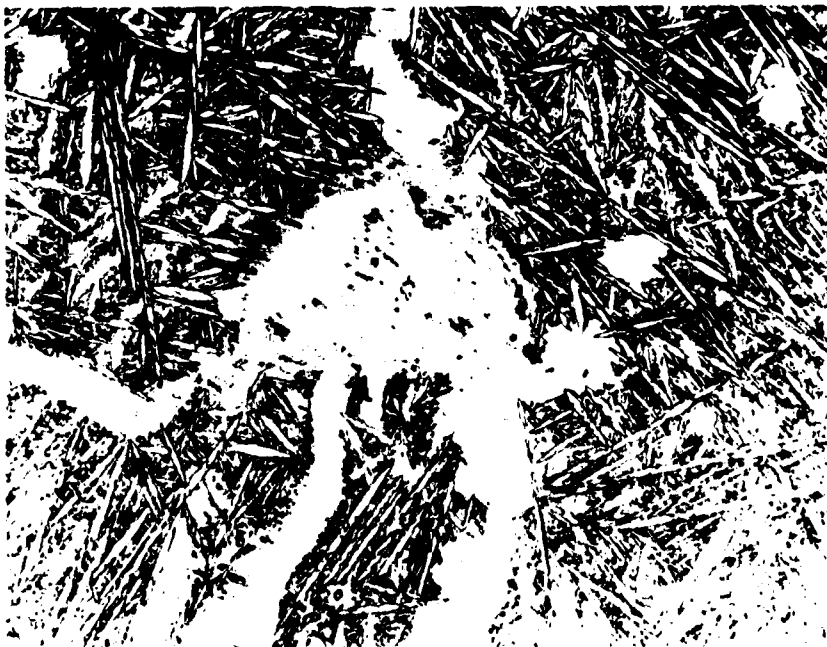
Figure 10b.   ETCHED (BRIGHT FIELD)   x 150
                                                       F4659

Figure 10.   Showing microstructure 8mm from
              bottom end of plunge quenched bar.   R812/4

Figure 11a. CROSSED POLARS x 150
F4650
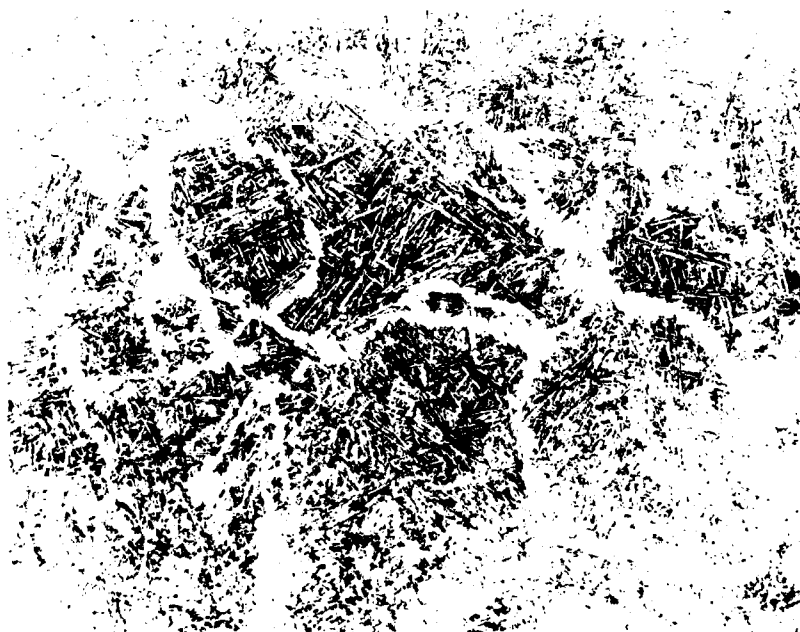
Figure 11b. ETCHED (BRIGHT FIELD) x 50
N9237

Figure 11. Showing general microstructure 60mm
from bottom end of plunge quenched bar.
Note the single phase delineation of
prior γ grain boundary, marked 'A' in
Figure 11a. R812/4
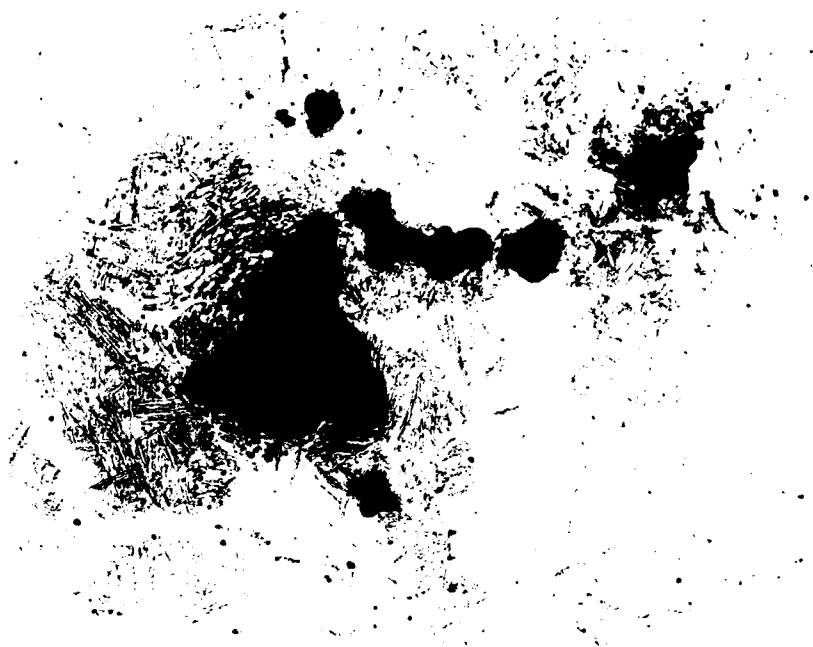
Figure 12.   Showing pores near centreline of plunge   x 150
              quenched bar, 60mm from bottom end.   N9056
                    ETCHED (BRIGHT FIELD)
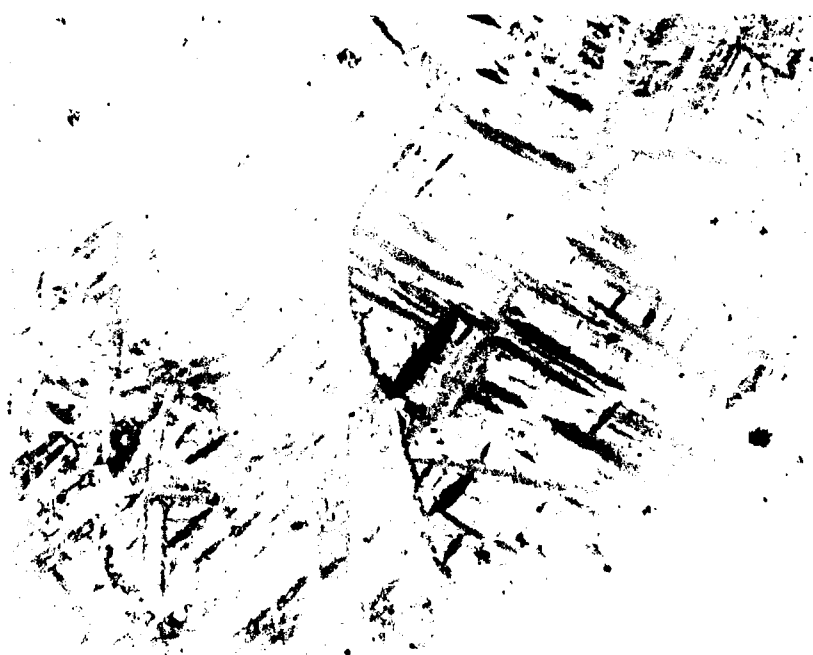
Figure 13.   Showing martensitic α' microstructure close   x 150
              to outer edge, 60mm from bottom end of   F4649
              plunge quenched bar.
                        CROSSED POLARS   R812/4

Figure 14. Showing microstructure 2 mm from end of   x 150
            end quenched bar. Note the granular   F4253
            nature of the regions adjacent to prior
            γ grain boundaries.
                 ETCHED + CROSSED POLARS

Figure 15. Showing microstructures 10mm from end of   x 150
            end quenched bar.   F4212
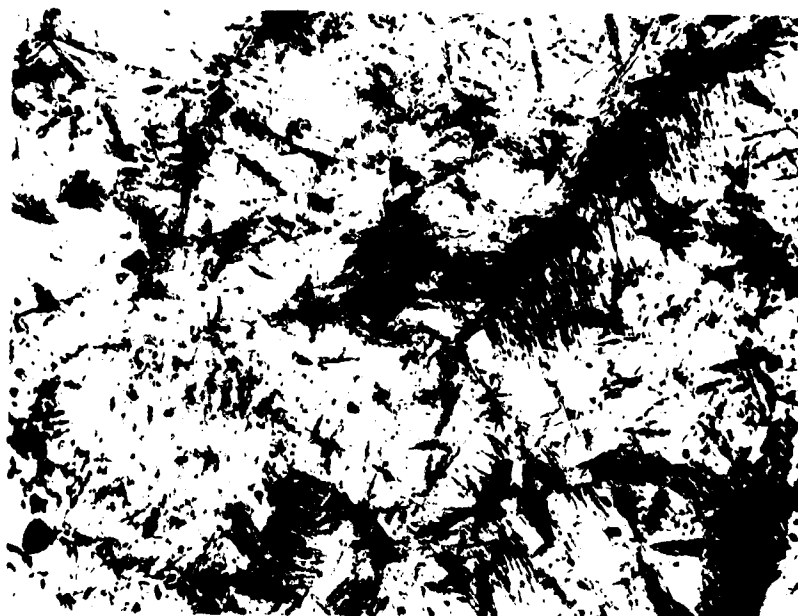   ETCHED + CROSSED POLARS

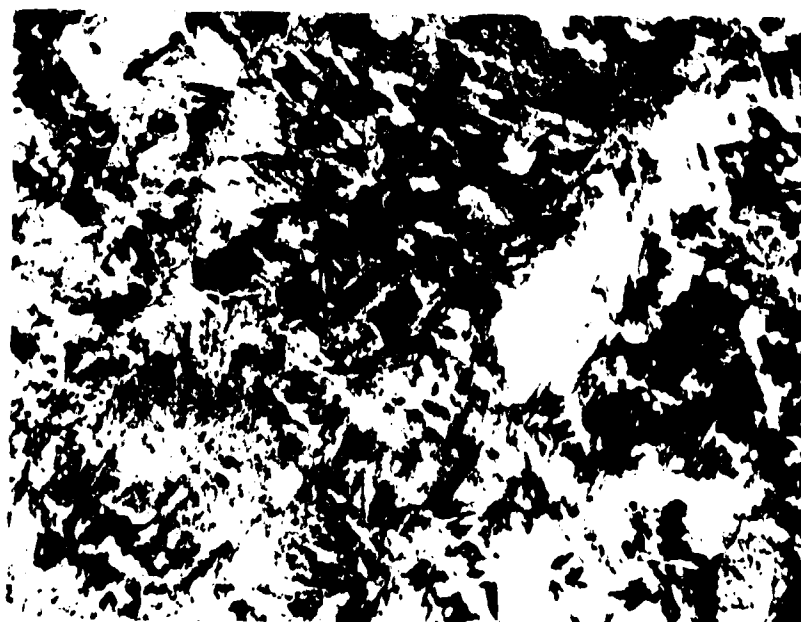Figure 16a.

CROSSED POLARS

x 150

F4224

Figure 16b.

ETCHED

(BRIGHT FIELD)

x 150

F4257

Figure 16c.

ETCHED +

CROSSED POLARS

x 150

F4258

Figure 16. Showing microstructure 50mm from end of
end quenched bars.

R812/4

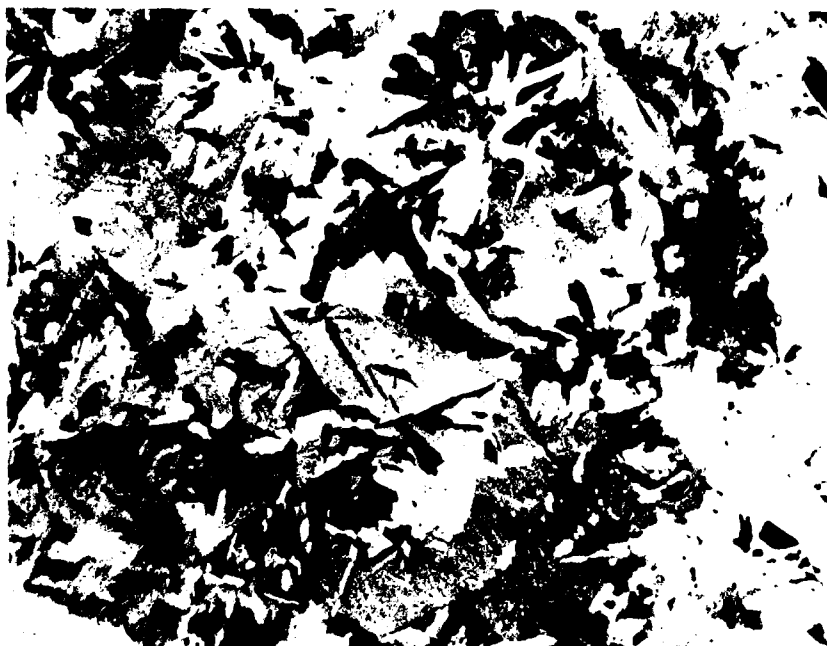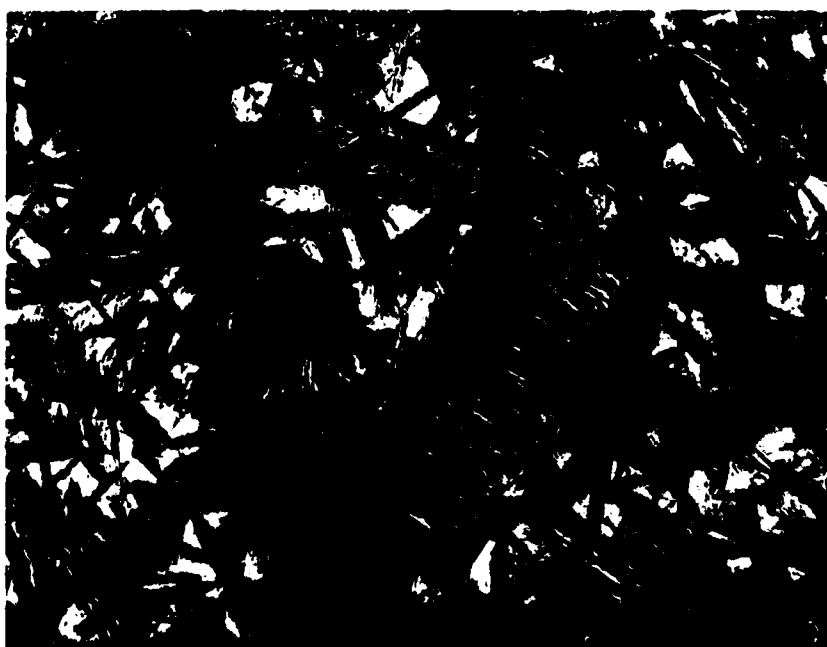Figure 17a.   CROSSED POLARS   x 150
                                                                     F4671

Figure 17b.   ETCHED (BRIGHT FIELD)   x 150
                                                                        F4259

Figure 17.   Showing microstructure 70mm from end of
                  end quenched bar.   R812/4

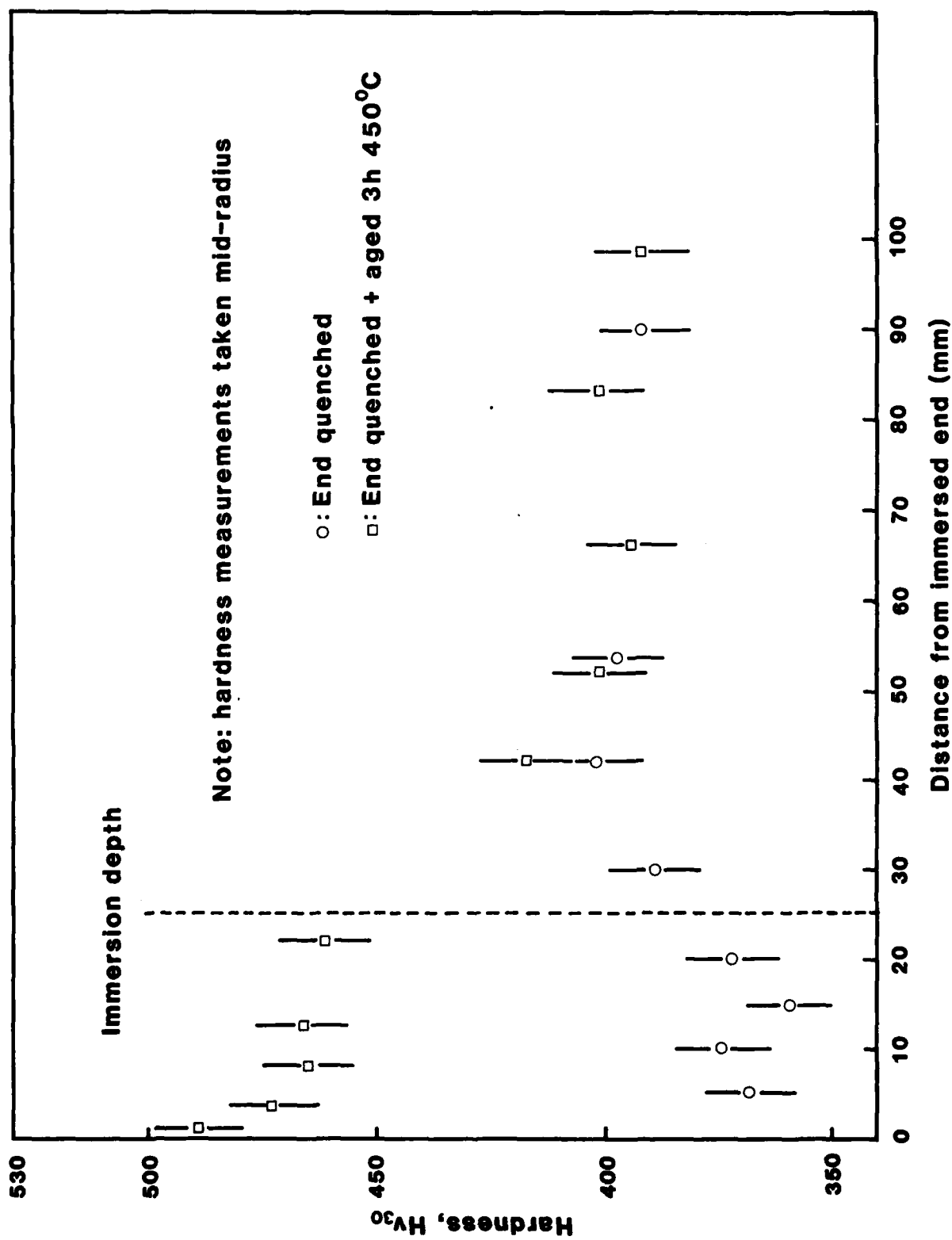Figure 18 Variation of Vickers hardness with distance in end quenched bars

Figure 19a.   CROSSED POLARS   X 150
                                                                 F4673

Figure 19b.   ETCHED (BRIGHT FIELD)
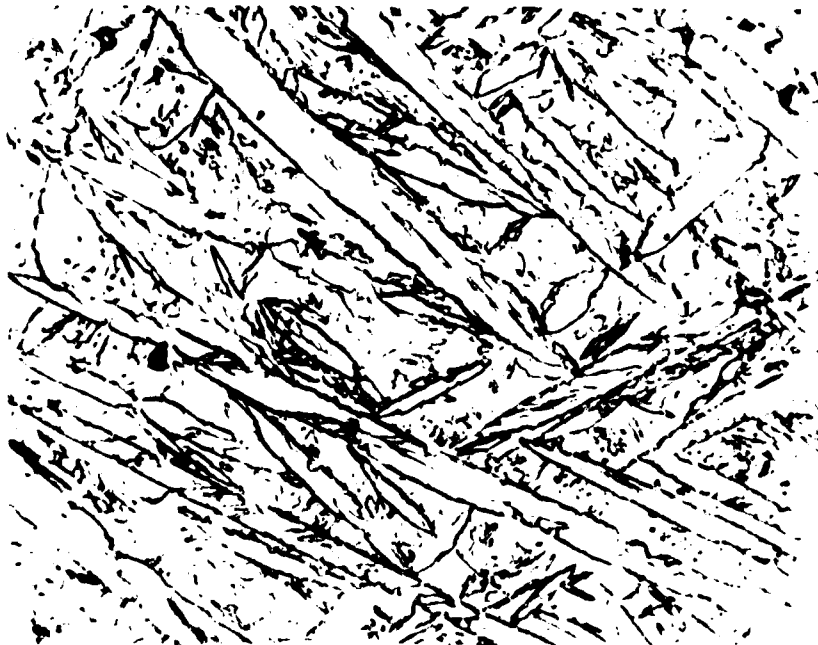   X 150
                                                                 F4414
Figure 19.   Showing microstructure 10mm from end of bar
              immersed at 100mm/s.
                                                                 Ref. 4

Figure 20.   Showing martensitic structure 10mm from   x 750
             end of bar immersed at 100mm/s.   F4415
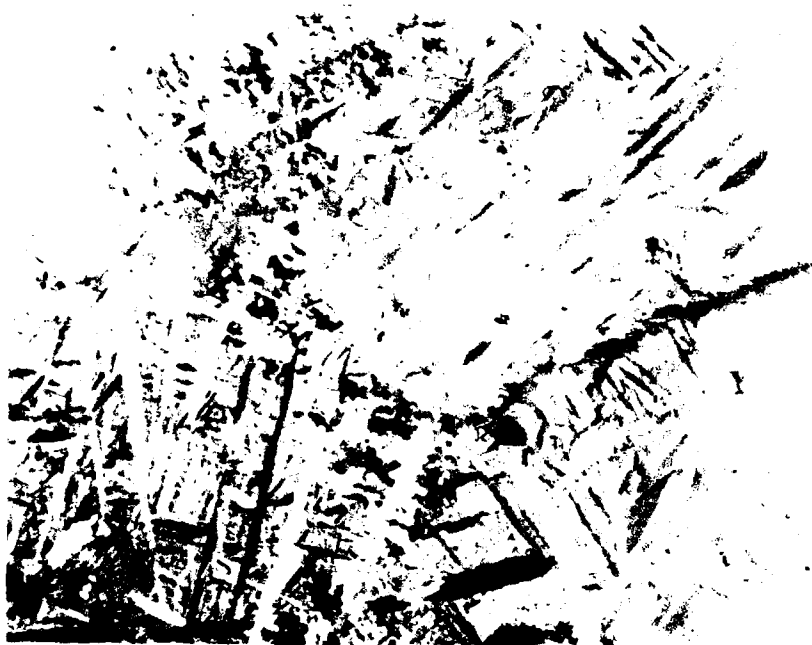   ETCHED (BRIGHT FIELD)

Figure 21. Showing microstructure 35mm from end of bar immersed at 100mm/s.
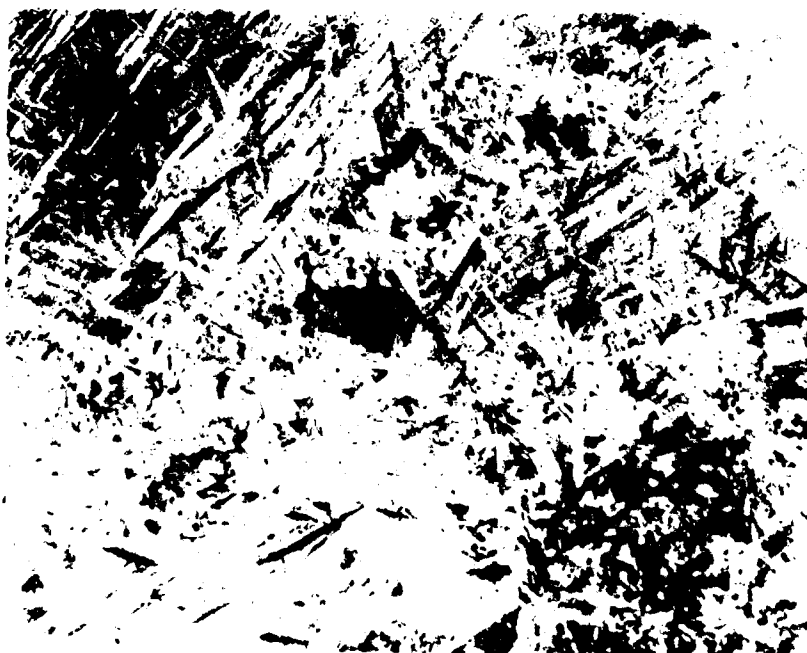CROSSED POLARS

x 150
F4674

Figure 22. Showing microstructure 50mm from end of bar immersed at 100mm/s.
CROSSED POLARS

x 150
F4410

R812/4

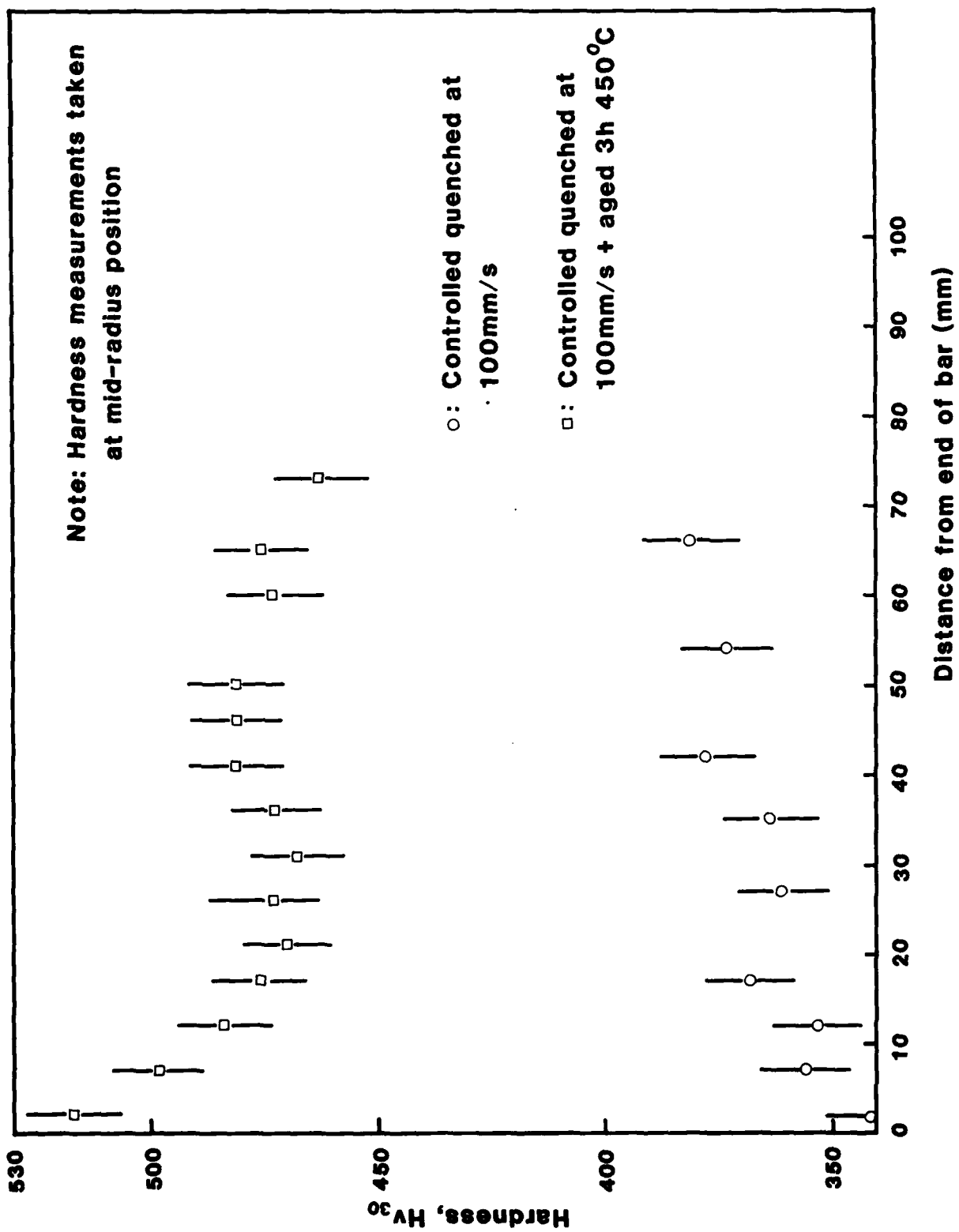Figure 23 Variation of hardness with distance from end of bar

Figure 24a.   CROSSED POLARS   x 150
                                                                 F4665

Figure 24b.   ETCHED (BRIGHT FIELD)   x 150
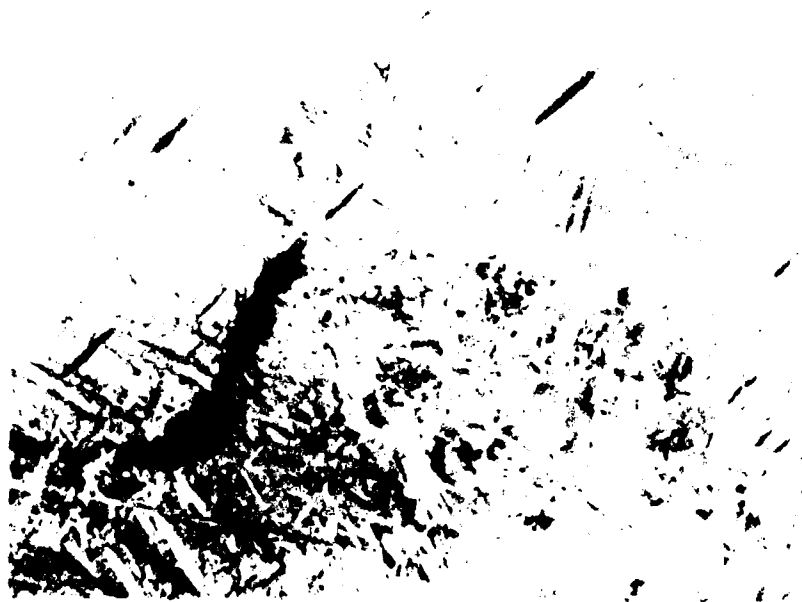   F4668

Figure 24.   Showing microstructure 30mm from end of
             bar immersed at 10mm/s.   B912/4

Figure 25. Showing structure 35mm from end of end quenched   x 150
            bar after ageing 3 hours 450°C.   F4670
                        CROSSED POLARS

Figure 26. Showing structure 70mm from end of end quenched   x 150
            bar after ageing 3 hours 450°C.   F4669
                        CROSSED POLARS

R812/4
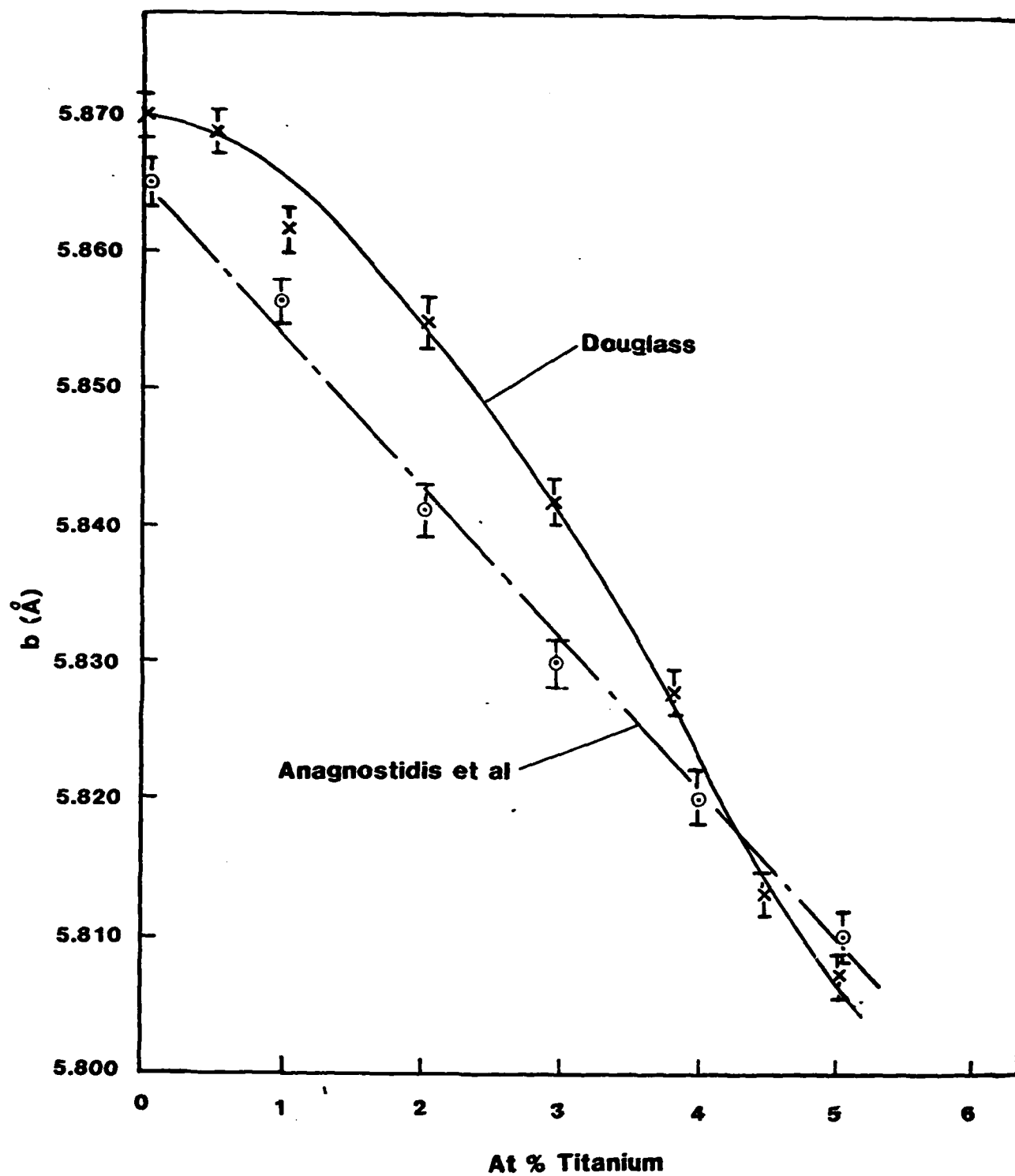
Figure 27 Variation of 'b' lattice parameter with composition according
to Anagnostidis et al[13] and Douglass[14]